JOURNAL OF APPLIED ELECTROCHEMISTRY 22 (1992) 172–178

Phase-structure analysis of brass by anodic linear-sweep voltammetry

J. STEVANOVIĆ
Institute of Electrochemistry — ICTM, Njegoševa 12, 11000 Beograd, Yugoslavia

LJ. SKIBINA
Faculty of Chemistry, Rostov State University, Rostov on Don, USSR

M. STEFANOVIĆ
DP 'Petar Drapšin', 11400 Mladenovac, Yugoslavia

A. DESPIĆ
Faculty of Technology and Metallurgy, University of Beograd, Karnegijeva 4, 11000 Beograd, Yugoslavia

V. D. JOVIĆ
Institute of Technical Sciences of the Serbian Academy of Science and Arts, 11001 Beograd, P.O. Box 745, Yugoslavia

Received 2 January 1991; revised 23 May 1991

Anodic linear-sweep voltammetry (ALSV) was applied to electrodeposited alloy layers and to metallurgically obtained Cu–Zn alloys of different composition and structure. Metallurgically obtained samples covered the range of composition in which α, (α + β), β and (β + γ) intermediate phases were detected by X-ray. The ALSV of samples containing less than 30 wt % Zn exhibited a single peak at -0.08 to -0.1 V/SCE before massive dissolution, starting at about -0.05 V/SCE. The presence of the γ-phase gave another peak at a significantly more negative potential (-0.25 to -0.35 V/SCE). The ALSV of electrodeposited alloys were significantly more complex than the former, depending on the deposition potentials, with peaks attributable to pure Zn, to the ε-phase, to the η-phase as well as to the α-phase, present in most cases and dissolving at potentials similar to that of pure Cu. ALSV was shown to be a reliable and practical method for a fast determination of both the composition and the phase structure of electrodeposited brass.

1. Introduction

Anodic dissolution of binary alloys has been extensively investigated [1–5] mainly following a dispute over selective as opposed to a simultaneous dissolution of the components. Relatively recently it was realized that the dissolution process may be very sensitive to the potential of such an alloy in electrolyte solution and that this sensitivity may be used for characterizing the state of the components in different phases of alloy [6–9]. Anodic linear sweep voltammetry (ALSV) was found to be particularly suitable for such an investigation, as the scanning of the potential over a range between the point of zero current as the negative limit and a massive anodic reaction as the positive one, results in a current response (typically with current peaks) indicating selective anodic oxidation of alloy components.

In special cases of very high energies of alloying, or highly inhibited anodic charge transfer, an alloy (e.g. copper–nickel alloys) may behave as "more noble" than either of the parent metals, i.e. start dissolving at potentials more positive than the dissolution potentials of either of the pure metals. In such cases simultaneous dissolution of both components occurs. In most cases, however, the component of the alloy having a more negative standard electrochemical potential than the other component (the 'negative component') starts dissolving selectively at a potential anywhere between that of the dissolution of the pure negative component and that of the positive one.

As the amount of that substance which is released from the alloy is limited, because of the inhibited diffusion in the solid state, the current goes through a maximum and subsides virtually to zero if the potential is held at this value or if it is changed slowly in the positive direction. The "positive component" starts dissolving at a potential virtually equal to that of the pure metal indicating that either the crystal structure of the alloy collapsed into that of the latter, or that a dissolution/reprecipitation mechanism took place with that component in the course of dissolution of the alloy. If the alloy sample is thick enough the massive dissolution of the positive component causes

0021-891X/92

Table 1. Metallurgical alloy composition

Sample no.	*wt % Cu*	*wt % Zn*	*wt % Pb*
1	88.0	12.0	–
2	79.2	20.6	–
3	70.9	29.1	–
4	63.2	36.7	–
5	58.0	42.0	–
6	52.3	47.6	–
7	47.7	52.3	–
8	42.0	57.2	–
9	38.0	61.4	–
10	58.4	38.6	2.5

a virtually unlimited rise of the current and, hence, makes for the positive limit of the potential scan. If the alloy is in the form of a thin film on an inert substrate (obtained by electrodeposition, PVD or CVD) the dissolution current of the positive component also exhibits a maximum and subsides to zero. As the peak potential is characteristic of the state of the negative component in the alloy and the quantity of electricity under the peak directly reflects the quantity of the component in such a state, the analysis of the voltammogram can be used both for a phase-structure determination and for a quantitative estimate of the phase-composition.

In the present communication results are reported on the use of the method for analysing copper-zinc alloys of different compositions obtained both in the form of thin films electrodeposited onto an inert electrode as well as in the form of bulk alloys cast in a metallurgical process.

2. Experimental details

ALSV was performed on alloy samples in a standard electrochemical cell using a potentiostat (PAR 273) with built-in programmer (sweep generator). The cell contained a platinum wire counter-electrode and a reference standard calomel electrode (SCE) electrolytically connected with the electrolyte in the cell via a Luggin capillary.

Thin films of alloys were obtained by depositing the metal potentiostatically (galvanostatically) onto glassy-carbon discs from a bath containing both Zn^{2+} and Cu^{2+} ions, at different cathodic potentials (currents) and to different thickness (different time of deposition). The deposition was carried out from the standard pyrophosphate bath [10] at room temperature.

Metallurgical samples with compositions shown in Table 1, were prepared (by courtesy of "Petar Drapšin" Mladenovac) of high purity zinc and copper by melting the components together and casting them into a cylindrical mold. One sample was taken from a commercial stock (sample 10).

The samples were machined into small cylinders, 10 mm in diameter, and cut into discs 5 mm thick. The latter were made into electrodes by soldering a wire contact at the back and sealing all the sides but one face with epoxy resin. The samples were polished mechanically to a mirror finish, washed in warm water and degreased in alcohol.

Electrodeposited and metallurgically cast samples were investigated in 0.3 M Na_2SO_4 electrolyte made of analytical grade salts and triply distilled water. The ALSVs were obtained at low sweep rates (5–10 mV s^{-1}) at 25° C without stirring.

The cast alloy samples were also submitted to X-ray analysis of the phase structure. An X-ray diffractometer Seifert (Hamburg, FRG) was used. Auger electron spectroscopy (RIBER) as well as atomic absorption analysis were also applied to determine the chemical composition of the electrolytic deposits.

3. Results

3.1. *Electrochemically deposited samples*

3.1.1. Cathodic deposition. A typical set of potentiostatic transients for cathodic deposition from the pyrophosphate bath is shown in Fig. 1(a). Transient phenomena, within the 50 s potential steps, are observed at potentials less negative than −1.0 V and more negative than −1.6 V/SCE in the same electrolyte. Steady-state polarization curves could be extracted from the flat portions of the transients, except at potentials more negative than −1.6 V, and are shown in Fig. 1(b). It may be seen that deposition of the alloy starts at significantly less negative potentials than either that of pure zinc or of pure copper obtained in the same way but from electrolytes containing only one corresponding ion. Three additional features should be noted: (a) significant deposition (at $j_c > 0.1$ mA cm^{-2}) occurs only at potentials more negative than −0.6 V; (b) a tendency towards a limiting current density exists in the pyrophosphate electrolyte at potentials more negative than −0.6 V and (c) a rather sharp increase starts at −0.8 V, i.e. at significantly less negative potentials than the steady increase with time exhibited in the transients of Fig. 1(a). Thus, one may expect reasonably fast and good deposition to occur in the potential range between −0.7 and −1.5 V/SCE.

Electrodeposited alloy layers were obtained from pyrophosphate electrolyte with three different concentrations of the depositing ions: (a) 0.01 M Cu^{2+} + 0.1 M Zn^{2+}; (b) 0.02 M Cu^{2+} + 0.05 M Zn^{2+} and (c) 0.05 M Cu^{2+} + 0.1 M Zn^{2+}. Quantities of electricity passed for cathodic deposition ranged between 0.3 and 10 C cm^{-2}. If a current efficiency between 0.5 and 0.25 is assumed (*cf.* below), the thickness of the layers ranges between 30–60 nm and 1.2–2.4 μm.

3.1.2. ALSV of electrodeposited alloy layers. Depending on the deposition potentials different ALSVs were obtained. ALSVs of alloys deposited in the potential region between −0.6 V and −1.1 V/SCE in the same bath, 'low potential region', exhibited a single peak (curves 0, Fig. 2a). The peaks coincide with peak potential for the dissolution of pure copper. However,

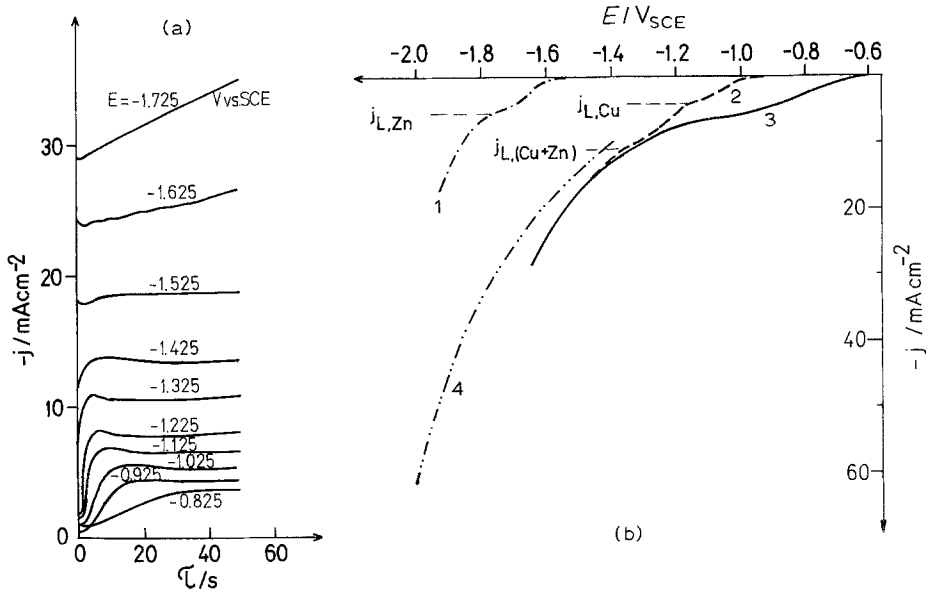

Fig. 1. (a) A set of potentiostatic transients for the deposition of the alloy from the pyrophosphate bath containing 0.02 M Cu^{2+} and 0.05 M Zn^{2+} ions on glassy carbon rotating disc electrode at 1000 r.p.m. at different potentials; (b) steady-state current density-potential relationship for cathodic polarization in the pyrophosphate bath containing (1) only 0.05 M Zn^{2+}, (2) only 0.02 M Cu^{2+}, (3) 0.05 M Zn^{2+} + 0.02 M Cu^{2+} and (4) 0.1 M Zn^{2+} + 0.01 M Cu^{2+}. *Note*: j_L, Cu — diffusion limiting current for Cu^{2+}, j_L, Zn — diffusion limiting current for Zn^{2+}.

the amounts of metal dissolved, reflected in the quantities of electricity under the peaks, are found to be significantly higher than those which were dissolved after the deposition at the same cathodic potential from the same bath, but containing only Cu^{2+} ions at the same concentration. Analysis by atomic absorption as well as ESCA–Auger analysis of the alloy layers revealed the presence of large amounts of zinc.

At deposition potentials more negative than −1.2 V/SCE in the same bath ('high potential region') significantly more complex ALSVs are found as exemplified by Fig. 2a and b.

In relatively thick deposits, towards the upper limit of thickness of the investigated samples, up to five peaks (or shoulders) are found (Fig. 2b). The potential of the first peak, E_A, is found to correspond to the peak-potential of dissolution of pure zinc.

In relatively thin deposits, obtained during a short deposition period (up to 50 s, Fig. 2a), peak E is the most dominant at all deposition potentials in the high deposition potential region. However, additional peaks, though an order of magnitude smaller, are found at E_C and E_D, with the peak C going through a

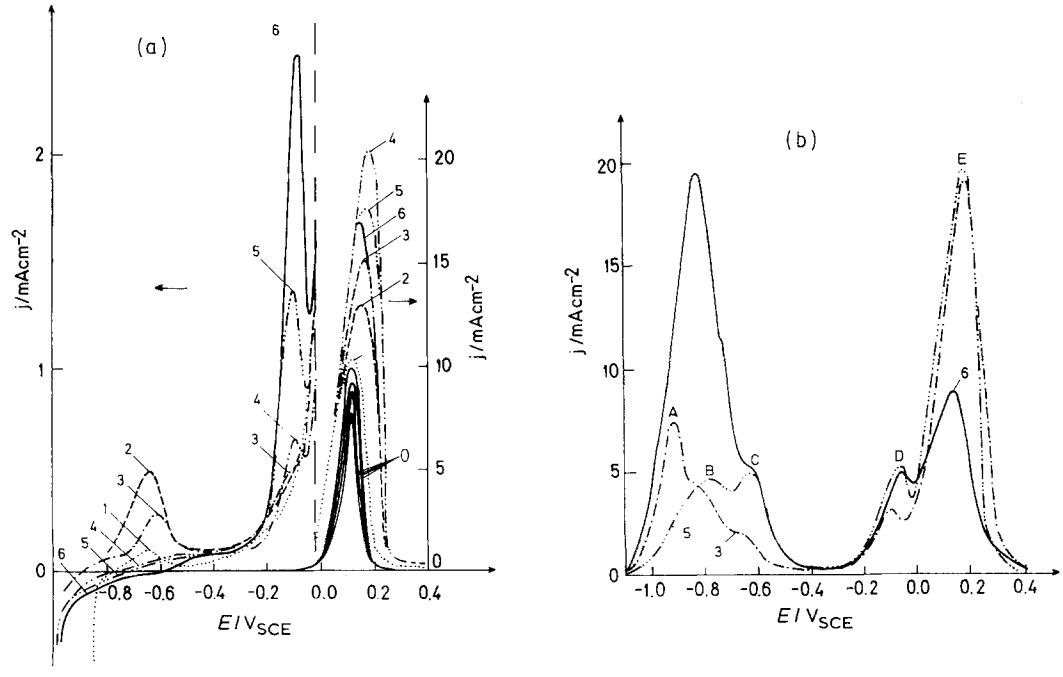

Fig. 2. ALSVs of dissolution (sweep rate 5 mV s^{-1}) of alloy layers deposited from the pyrophosphate bath at potential (given against SCE): −0.6 to −1.1 V (0); −1.2 V (1); −1.3 V (2); −1.4 V (3); −1.6 V (4); −1.8 V (5) and −1.9 V (6) (a) for 50 s and (b) to a thickness of about 0.6 μm.

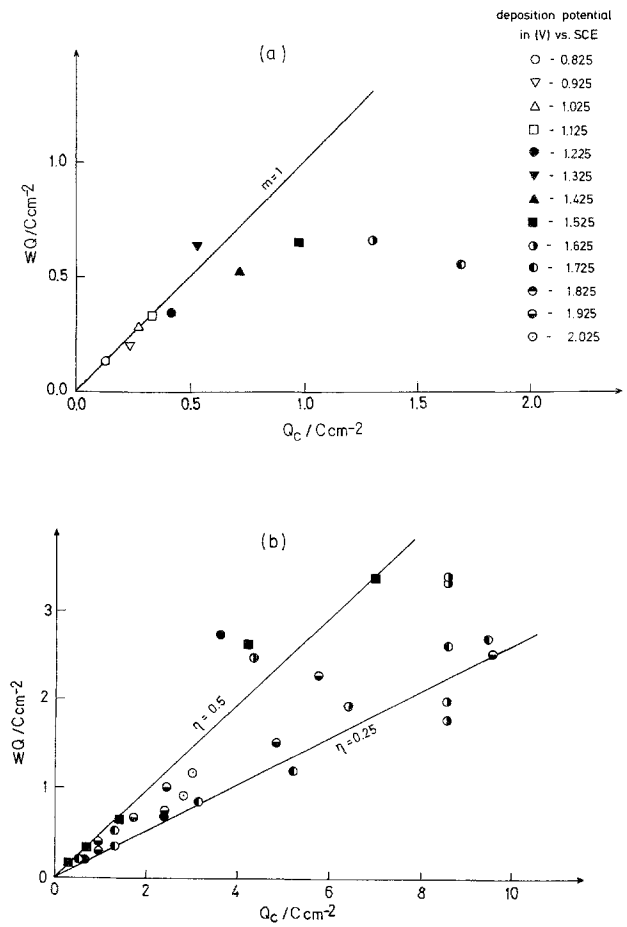

Fig. 3. The sum of charge under all the peaks in the ALSVs obtained for alloys deposited at different cathodic potentials (marked in the figure), as a function of the corresponding cathodic deposition charge: (a) short deposition time (50 s) and (b) after extended deposition.

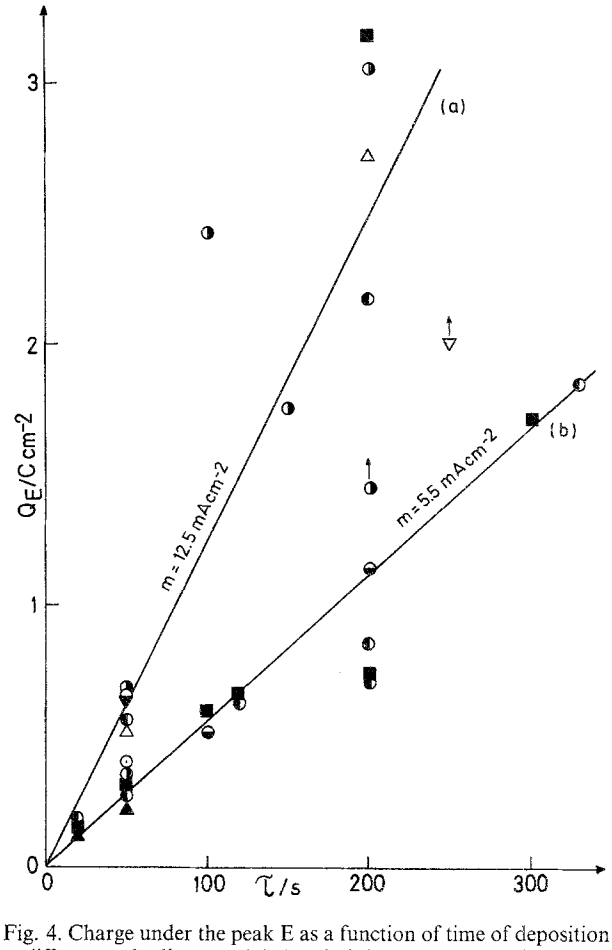

Fig. 4. Charge under the peak E as a function of time of deposition at different cathodic potentials (symbols in points same as in Fig. 3). Concentration of Cu^{2+}: (a) 0.02 M; (b) 0.01 M.

maximum and then subsiding and with peak D increasing with increasingly negative deposition potential.

The total anodic charge was obtained by integrating the entire ALSVs. Plotted against the cathodic charge passed during deposition (Fig. 3) it gives the current efficiency from the slope, if equal charge transfer in deposition and dissolution per atom is assumed.

At short deposition times (50 s), i.e. for very thin deposits, the efficiency is seen (Fig. 3a) to approach 100% at low cathodic potentials and to fall to about 50% in the high cathodic potential region. In thicker deposits in the high cathodic potential region (Fig. 3b) it is seen to be rather low, i.e. between 50% and 25%.

The charge under the dominant peak E is found not be depend on deposition potential, as seen in Fig. 4, but only on the time of deposition. It appears, therefore, that the phase dissolving with that peak-potential is depositing at one and the same average current density. The slope of Fig. 4 indicates this to be 5.6 mA cm^{-2} and 12.5 mA cm^{-2} for two different concentrations of Cu^{2+}, which is of the order of the diffusion limiting current density for the deposition of the alloy indicated by Fig. 1(b).

The peaks B and C appear regularly with thicker deposits, though with poor reproducibility in terms either of peak potential or charge under the peaks, making the separation of the peaks difficult. Nevertheless, it could be said that E_B is found in the region of -0.9 to -0.7 V/SCE, while E_C is between -0.8 and -0.5 V/SCE depending on the charge under the peaks. The charge under both peaks is seen in Fig. 5a not to depend on deposition potential, but rather on the total cathodic charge passed during deposition, indicating a current efficiency of formation of the phases concerned, of about 6.5%.

Contrary to that, the amount of charge under the peak A is seen to depend on deposition potential (Fig. 5b) showing two different current efficiencies for deposition of phase ascribed to the peak A.

3.2. *Cast alloy samples*

Nine cast alloy samples were investigated ranging in composition from 12 to 61 wt% of zinc. The X-ray diffractograms, shown in Fig. 6 demonstrate that samples covered a number of phase structures from a pure α-phase (samples 1–3), (α + β)-phases (samples 4 and 5), β-phase (sample 6), (β + γ)-phases (samples 7, 8 and 9) with increasing content of the γ-phase. The sample from the commercial stock also gave Pb peaks, as it contained 2.5 wt% of Pb.

ALSV recordings for samples corresponding to the X-ray diffractograms of Fig. 6 are shown in Fig. 7.

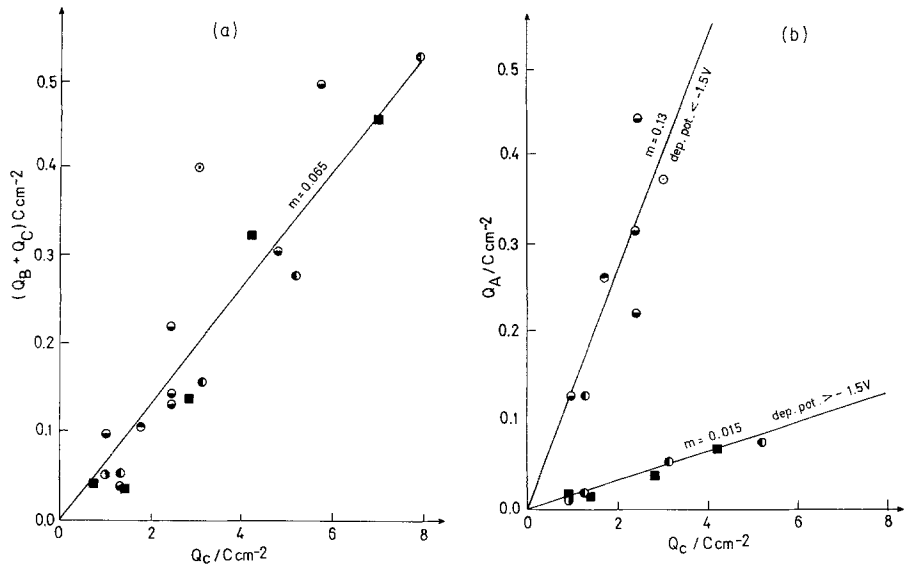

Fig. 5. The sum of charges Q_B and Q_C – (a) and the charge Q_A – (b) as a function of the cathodic charge used in the deposition of the alloy (symbols in points same as in Fig. 3).

The voltammograms for the samples 1 to 5 were found to exhibit a single peak at a peak potential of -0.07 V/SCE virtually independent of the sweep rate and with a peak current and the charge under the peak increasing both with the sweep rate and with the increase in zinc content. Samples 6 to 8, consisting predominantly of the β-phase, exhibited a shift of the peak-potential by some 20 mV in the negative direction. Sample 8 exhibited another peak at a peak potential of -0.32 to -0.23 V/SCE depending on the sweep rate. Sample 9 exhibited a single peak between -0.6 and -0.29 V/SCE shifting in the positive direction with increasing sweep rate, and a shift of the beginning of massive dissolution to potentials at which the single peak in samples 1 to 5 starts to form. For the commercial sample containing lead an

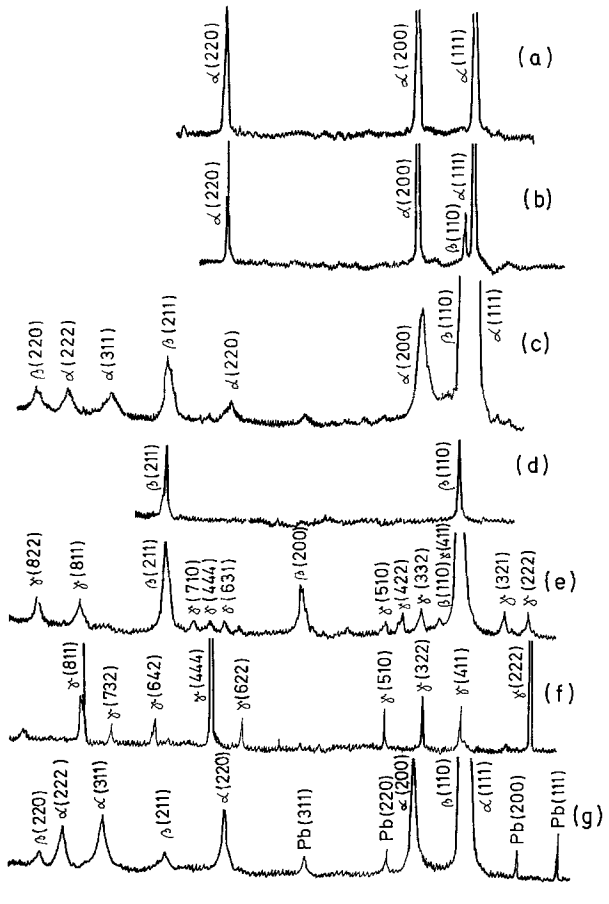

Fig. 6. X-ray diffractograms of cast alloys: (a) sample 1 (same for 2 and 3); (b) sample 4; (c) sample 5; (d) sample 6; (e) sample 8 (same for 7); (f) sample 9; (g) commercial alloy.

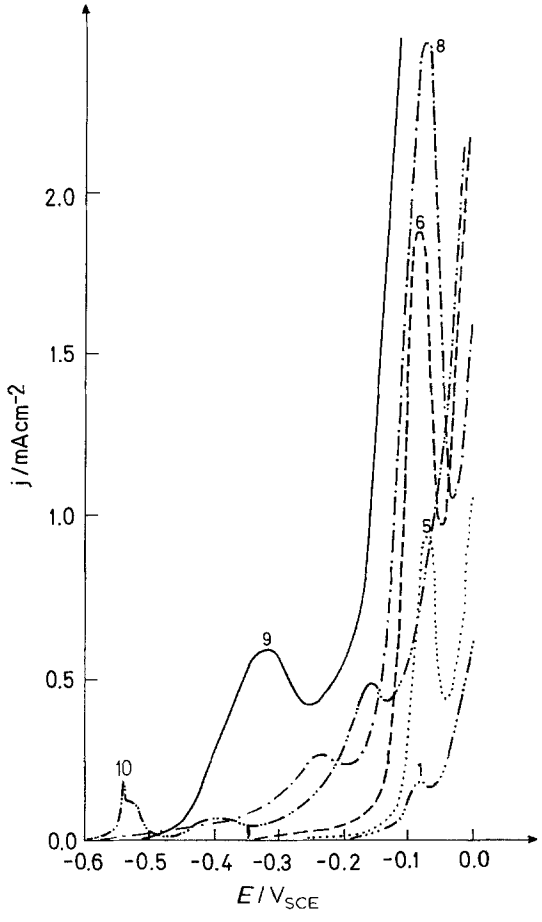

Fig. 7. ALSVs for the set of cast alloy samples (denoted at peaks) at one and the same sweep rate of 10 mV s^{-1}.

Table 2. Zinc content of electrochemically deposited alloy as a function of cathodic overpotential

Overpotential E/V_{SCE}	−0.925	−1.025	−1.125	−1.225	−1.325	−1.425	−1.525
at % Zn	10.5	26.1	34.6	45.2	57.5	69.1	82.6

additional sharp peak is obtained at a peak potential of −0.55 V/SCE.

4. Discussion

4.1. *Electrochemically deposited alloy*

4.1.1. Cathodic deposition. As already mentioned, the alloy is seen (Fig. 1b) to deposit upon cathodic polarization of the inert substrate, at more positive potentials than both parent metals. This obviously reflects either a more positive standard potential of the alloy, which may be due to a relatively large free energy of alloying (*cf.* thermodynamic considerations [9]), or faster kinetics, as a consequence of a catalytic effect of Zn^{2+} on the reduction of Cu^{2+} ions, or both. This phenomenon deserves detailed investigation.

Potentiostatic transients at potentials less negative than −1.0 V (Fig. 1a) exhibit delay in the increase of current typical of nucleation and growth of crystals on a foreign substrate, the attainment of the steady-state indicating coalescence of the crystals into a compact flat deposit. At potentials more negative than −1.6 V/SCE, the observed rise in current reflects surface roughening due to Zn^{2+} concentration polarization as a condition for the initiation of dendritic growth and powdery deposit.

Indeed, good quality, flat and bright deposits were seen below that potential limit, while above it (up to −2.8 V) a rougher and looser deposit was obtained. It is interesting to note that the diffusion limiting current of copper, indicated by the wave in Fig. 1b, is reached at −0.9 V and yet good quality deposits were obtained up to some 0.8 V more negative potentials. This indicates that the sharp rise in current at potentials more negative than −0.6 V must be due to the deposition of zinc into the alloy, covering copper and preventing dendritic growth.

An approximate zinc content could be calculated as the ratio between the excess of current over the Cu^{2+} diffusion limiting current and the total current. The result is given in Table 2. The electrochemical deposition provides good quality alloy with much larger zinc content than that obtainable by the metallurgical process and the presence of high-zinc content phases, as with the ε- and η-phase, may be expected.

Integration of the charge over the entire ALSV and comparison with the charge used in cathodic deposition (Fig. 3) gives the current efficiency of deposition. This is seen to be very high at low cathodic potentials and short deposition times indicating that hydrogen evolution is inhibited. However, at higher cathodic potentials and thicker deposits the situation is seen to change and the alloy deposition becomes a fairly inefficient process.

4.1.2. Phase-composition of the deposits

(*i*) *α-phase.* A single peak obtained in the ALSV of the alloy layers deposited in the potential range between −0.8 V and −1.1 V/SCE covers a significantly larger quantity of electricity than the corresponding peaks obtained in the potential range from the electrolyte containing only Cu^{2+} ions. As this peak is found to be dominant in the entire range of deposition potentials down to −1.9 V/SCE where there is no doubt that zinc is codeposited, one must conclude that it is the α-phase which dissolves at potentials coinciding with those of dissolution of pure copper. The fact that the quantity of the α-phase is virtually independent of the deposition potential and dependent on the deposition time only, indicates (a) that the α-phase formation is controlled by diffusion of the copper ions, and (b) that the α-phase takes up a constant amount of zinc, independent of the quantity of zinc deposited (excess zinc going into other phases). The fact that the calculated current densities of deposition taken from the slopes of Fig. 4 are larger than the diffusion limiting current for Cu^{2+} ions also indicates simultaneous deposition of zinc.

The simultaneous dissolution of zinc with copper is not unexpected, since in the relatively low zinc content of the α-phase (approx. 1 atom of zinc per 2 atoms of copper) the zinc atoms are held firmly in the face-centered cubic lattice dominated by relatively strongly bound copper atoms. This, however, handicaps the use of ALSV method for a qualitative and quantitative analysis of the α-phase in brass.

(*ii*) *β-phase.* The peak at the peak-potential E_D (Fig. 2) was identified (*cf.* below) as reflecting the presence of the β-phase. It is interesting to note that the amount of the β-phase found in the electrolytic brass is very small and obtained irregularly. When appearing, it does so at deposition potentials more negative than −1.4 V/SCE. The amount of the β-phase is about two orders of magnitude smaller than that of the α-phase. This makes the ALSV method more sensitive to the presence of that phase than any other conventional method of phase composition determination.

(*iii*) *ε- and η-phase.* The excess zinc, over that which could be accommodated in the α-phase, builds phases dissolving with peak-potentials E_C and E_B (Fig. 2b). Since the β-phase was found to dissolve at a less negative potential (*cf.* below), these peaks should pertain to the phases rich in zinc, as are the ε-phase and

the η-phase respectively which are not found in metallurgical brass.

(*iv*) *Pure zinc.* After deposition at potentials more negative than -1.5 V/SCE incidences of dissolution peaks at the potential E_A (Fig. 2b) are found, which coincides with the dissolution potential of pure zinc. It appears that in very fast deposition (at high current densities) pure zinc grains are sometimes nucleated and grow without alloying with copper. In some cases this appears in quite a significant amount. In rare incidences this is comparable to those of the α-phase.

It is interesting to note that pure zinc was never found in galvanostatic deposition, indicating a slower nucleation of the zinc phases, which is a general characteristic of galvanostatic vs potentiostatic deposition.

The above findings lead to several conclusions:
(a) in electrochemical deposition of brass the α-phase is the most dominant one under any conditions of deposition;
(b) in the samples where the amount of copper is insufficient to accommodate all the zinc in the α-phase, zinc-rich phases, or even pure zinc are deposited in parallel to the α-phase and in preference to the β- or γ-phase;
(c) inasmuch as the γ-phase was never found, in galvanostatic deposition the β-phase appears regularly in parallel to one zinc-rich phase and in addition to the α-phase;
(d) it appears that by controlling the deposition regime (deposition mode, potential or current density and time) one can obtain brass in the form of the α-phase alone, or with inclusion of small amounts of selected other phases which may modify its properties.

4.2.2. ALSV of cast alloys. The cast alloys gave ALSVs with well defined peaks before massive anodic dissolution took place at potentials more positive than -0.05 V/SCE.

(*i*) α-*phase.* The experience with the electrolytic alloys suggests that the α-phase dissolves at potentials at which massive dissolution takes place. In other words, as the bulk of the alloy consists of the α-phase, it dissolves at an ever increasing rate as the potential is driven positive, exhibiting no peak in the voltammogram. Hence, one must conclude that the ALSV method cannot be used for detecting a phase which constitutes the bulk of the metal, which in all investigated samples but sample 9 was the α-phase.

(*ii*) β-phase. In all samples in which the β-phase was detected by X-ray, a peak appeared in the ALSV at the foot or even up the slope of the increasing current of massive dissolution. Hence, it was reasonable to ascribe this peak to the β-phase. One should note that this peak, although covering a small amount of electricity, appeared also with samples in which the X-ray did not detect the β-phase. Hence, one could conclude that the ALSV presents a more sensitive method for phase detection than the X-ray analysis. It is only when the β-phase became predominant (sample 9), i.e. constituted a significant part of the bulk of the alloy, that no peak could be recorded because of an ever increasing current characteristic of bulk dissolution. Limits of detectability have yet to be established.

(*iii*) γ-*phase.* The appearance of another peak at potentials less negative than E_C (Fig. 2b) of the electrolytic deposit, coinciding with the appearance of the γ-phase in the X-ray diffractograms, leads to the conclusion that it must reflect the presence of the γ-phase. It is well separated from the peak of the β-phase and, thus, its presence in the alloy can be clearly seen.

Acknowledgements

The authors are indebted to the Research Fund of SR Serbia for material support. One of the authors (L.S.) is grateful to the University of Rostov on Don for leave of absence.

References

[1] H. Gerischer and H. Richert, *Z. Metallkunde*, **46** (1955) 681.
[2] J. O'M. Bockris, B. Rubin, A. Despić and B. Lovreček, *Electrochim. Acta* **17** (1972) 973.
[3] H. W. Pickering and P. J. Byrne, *J. Electrochem. Soc.* **116** (1969) 1492.
[4] H. W. Pickering and P. J. Byrne, *ibid.* **118** (1971) 209.
[5] J. E. Holiday and H. W. Pickering, *ibid.* **120** (1973) 470.
[6] S. W. Swathirajan, *ibid.* **133** (1986) 671.
[7] I. Petro, T. Mallat, A. Szabo and F. Hange, *J. Electroanal. Chem.* **160** (1984) 289.
[8] V. D. Jović, R. M. Zejnilović, A. R. Despić and J. S. Stevanović, *J. Appl. Electrochem.* **18** (1988) 511.
[9] V. D. Jović, A. R. Despić, J. S. Stevanović and S. Spaić, *Electrochim. Acta* **34** (1989) 1093.
[10] V. V. Bondar, V. V. Grimina and V. N. Pavlov, *Itogi nauki i techniki, Elektrokhimiya* Vol. **16**, Moscow (1980).